Measurement of Total Cross Sections for Electron Recombination With NO^+ and O_2^+ Using Ion Storage Techniques

F. L. WALLS AND G. H. DUNN

Joint Institute for Laboratory Astrophysics
National Bureau of Standards and University of Colorado, Boulder, Colorado 80302

The total cross section as a function of electron energy for recombination of electrons with room temperature NO^+ has been measured with a trapped ion technique. Measurements were made in the electron energy range 0.045–4 eV with an energy resolution between 0.045 and 0.120 eV, and the cross sections, which showed some structure, ranged from 1.25×10^{-14} cm² at the lowest energy to 1.7×10^{-16} cm² at the highest energy. Similar measurements were made on O_2^+, the species used to calibrate the apparatus geometry. A Maxwellian distribution of electron velocities was used with the measured cross sections to calculate rate constants, giving values extending to electron temperatures as high as 40,000°K. Comparison with previously measured rate coefficients at lower temperatures is quite satisfactory.

The high concentrations of NO^+ and O_2^+ in ionospheric regions between 90 and 250 km and the important role played by these ions in ionospheric modeling have led to an impressive number and variety of measurements and estimates for the recombination coefficients of these ions with electrons. The work has been nicely overviewed by *Bardsley and Biondi* [1970] in their review on dissociative recombination.

The excellent agreement between the O_2^+ investigations of *Mehr and Biondi* [1969] and those of *Cunningham and Hobson* [1972] as well as other less extensive experiments [*Sayers and Kerr*, 1957; *Kasner and Biondi*, 1968; *Mahdavi et al.*, 1971; *Plumb et al.*, 1972] leads one to conclude that the recombination coefficients for this ion are well known for $300°K \leq T_e \leq 4500°K$.

The situation for NO^+ is less satisfactory. *Weller and Biondi* [1968] and *Gunton and Shaw* [1965] varied total temperature, and each measured three values of the recombination coefficient for $200°K \leq T \leq 450°K$, thus obtaining agreement within stated uncertainties with each other and with other measurements [*Mahdavi et al.*, 1971; *Young and St. John*, 1966] made only at 300°K. At higher temperatures *Stein et al.* [1964] and *Lin and Teare* [1963] obtained estimates of recombination at 2900° and 5000°K, respectively, in shock-heated air under conditions for which NO^+ was presumed to be the major ion constituent. There is a large uncertainty associated with the measurements made at 2900° and 5000°K, thus leaving some doubt that one can reasonably estimate the recombination coefficient at temperatures greater than 450°K.

In this paper total recombination cross sections for NO^+ as a function of electron energy from 0.045 to 4 eV are reported. From these data, rate coefficients are calculated for electron temperatures extending up to 40,000°K, thus filling the gap cited above.

EXPERIMENT

Basically, the method used here is to introduce an electron beam of known energy into a cloud of trapped ions whose number is measurable. The depletion rate of the ions is quantitatively related to recombination.

The ion storage technique used is an outgrowth of earlier work on stored electrons [*Dehmelt and Walls*, 1968; *Walls and Stein*, 1973] and will be described in detail elsewhere. Briefly, the ions are contained in a cylindrically symmetric Penning-style quadrupole ion trap similar to the one described by *Byrne and Farago* [1965]. Containment in the $r - \theta$ plane is achieved by using a large homogenous magnetic field $\mathbf{B} = B_0\mathbf{k}$, where B_0 is usually 11.75 kG. Containment along the z axis is achieved by applying an electrostatic potential of the form $V = K(r^2 - 2z^2)$, which creates a harmonic well along the z axis. Each ion species has its own characteristic Z oscillation frequency given by

$$\omega_z = \{4V_0(q/m)[1/(R_0^2 + 2Z_0^2)]\}^{1/2} \quad (1)$$

where q/m is the charge to mass ratio, V_0 the voltage applied between the ring and the end caps, and $R_0 = 0.625$ cm and $Z_0 = 0.385$ cm are the inside dimensions of the trap. With $V_0 = 1$ V the normal well depth of 0.4 V is achieved.

The residence lifetime of ions in the trap ranges from minutes to hours, depending on species, and is limited by reactions with the background gas. Particularly inert ions like NH_4^+ live as long as 24 hours, thus demonstrating that diffusion from the trap is very slow. For NO^+ the residence time was about 40 min. Representative vibrational decay times of the $X^1\Sigma^+$ state of NO^+ are 73 ms for the 0–1 transition and 38 ms for the 1–2 transition (F. P. Billingsley, unpublished manuscript, 1974), so that one seems to be assured that the $X^1\Sigma^+$ ions are in the ground vibrational level by the time recombination measurements commence about 600 s after formation. Lifetimes of the $a^3\Sigma^+$ excited electronic state of NO^+ do not seem to be known, but comparison of analogous transitions in the isoelectronic molecules N_2 [*Zipf*, 1969] and CO [*Anderson*, 1971] leads one to expect lifetimes of a few seconds or less. One might then expect that only $X^1\Sigma^+$ electronic states will be populated, but to insure this, NO^+ ions are formed by electron bombardment of NO with electrons of only 14-eV energy, less than enough to make $a^3\Sigma^+$ ions. In O_2^+ the vibrational lifetimes do not seem to be known but may be expected to be 10^6–10^7 s if they are typical of homonuclear species [*Bates and Poots*, 1953]. Collisional relaxation times are not well known for ion-neutral and ion-ion collisions, but *Takayanagi* [1964] predicts about 3×10^9 s for O_2^+ relaxation on O_2 for the densities encountered here ($\sim 10^{-10}$ torr). It thus appears that O_2^+ vibrational populations will be those characteristic of the formation process.

The $a^4\Pi_u$ electronic state of O_2^+ is expected to be long lived with an unknown lifetime, but the analogous transition to the ground state in NO has a lifetime of 0.16 s [*LeFebvre-Brion and Guerin*, 1968], so that electronic states probably should have decayed by the time of a measurement. In the case of O_2^+, ions were created by the bombardment of O_2 by electrons of both 14 and 33 eV, and a difference in recombination was found, as is discussed later.

After the ions are created in the trap, as is discussed above, Coulomb collisions between ions establish a Maxwellian distribution of kinetic energies in $\sim 10^{-2}$ s. Evaporation from the trap and other interactions cause the ions to cool down to room temperature in several minutes. The useful ion population is limited by space charge to about 10^4 ions, corresponding to a density of about $10^6/cm^3$.

The ions are nondestructively detected by measuring the noise power in the image currents to one end of the trap [*Dehmelt and Walls*, 1968], induced by their thermal motion in the axial harmonic well. Individual ion species are manifest as peaks in the noise power spectrum at the Z oscillation frequencies ω_z given in (1). The area under a peak is proportional to the product of ion number N_i and temperature T_i. If either N_i or T_i is effectively constant over the time of an experiment, then one can investigate any phenomenon that can be coupled to the other parameter. A phenomenon that couples to T_i with constant N_i is cyclotron resonance, which gives a q/M resolution of two parts in 10^4 and has been used to establish definitely the identity of O_2^+ and NO^+ in these measurements.

Electrons are introduced into the trap from either of two sources. In the first source, the low-resolution gun, electrons from an indirectly heated cathode are accelerated through a series of apertures into the trap with trajectories along the magnetic field lines. The second source, a high-resolution gun, is a trochoidal monochromator similar to that described by *Stamatović and Schulz* [1970]. Electron energies and energy distributions are determined by retarding potential measurements made by varying the potential of the electron gun relative to that of the trap. This procedure determines only the energy associated with velocities along the z axis. Measurements on the low-resolution gun used for most of the recombination measurements here indicate an axial energy distribution about 0.110 eV wide with a fairly long high-energy tail. The high-resolution gun used for measurements on NO^+ from 0.045 to 0.200 eV gives a beam with an axial distribution about 0.03 eV wide. Tests and modeling have led us to conclude that for the low-resolution gun, up to 0.045 eV could be associated with velocities perpendicular to the z axis. The corresponding value for the high-resolution gun is 0.010 eV. In using either gun the electron energy is both shifted and broadened by about 0.015 eV, owing to variation of the potential in the trap where the ions are encountered.

The data on recombination were taken by first measuring the integral under a given q/M peak relative to the background level versus time in the absence of electrons. This measurement yields the natural decay period τ_n, or ion residence time in the trap. Electrons at a well-defined energy are then run through the trap until a measurable number of ions is lost, after which τ_n is again measured. Figure 1 shows such a recombination measurement on NO^+ at an electron energy of 0.045 eV. This process is repeated a number of times at different electron energies, and the cross section is calculated from

$$\sigma = (e/i_e)A'[(1/t_e)\ln(N_1/N_2) - (1/\tau_n)] \qquad (2)$$

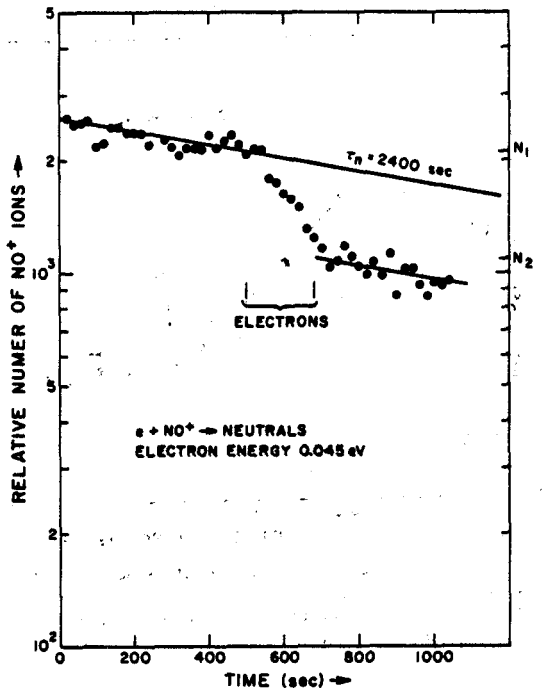

Fig. 1. Recombination data for NO^+ at an electron energy of 0.045 eV. The data from 500 to 700 s show the decay of ion signal in the presence of electrons. Measurements at other times demonstrate residual decay mechanisms.

where i_e is the electron current, t_e is the time that the current is on in the trap, N_1 and N_2 are the number of ions before and after introducing electrons, respectively, and A' is a geometric quantity depending on the overlap of the electron beam with the ion cloud.

Quantities in (2) are all readily measurable except for A', which in a simple geometric modeling is just the area of the ion cloud as seen by the electron beam. This quantity may be estimated on the basis of such modeling but only to within a factor of 2 or 3. An alternative procedure is to measure A' by measuring quantities in (2) for a process where σ is known. The process chosen to use in a measurement of A' is recombination with O_2^+, where in fact σ is not known but the recombination coefficient,

$$\alpha = \int_0^\infty \sigma(v)vf(v)\,dv \qquad (3)$$

has been well measured by a number of investigators, as was noted in the introduction. In this equation, $f(v)$ is the Maxwellian distribution of electron velocities v. Thus cross sections measured for O_2^+, as was done in (2), are used in (3) to calculate the α, which are in turn compared with measured values of the recombination coefficient to determine A'. The value so determined is about 1.9 times the value estimated from a simple geometric model.

Except for small corrections due to different cyclotron radii the value of A' is not expected to vary significantly from one ion species to another if creation conditions are the same. For NO^+ and O_2^+, this correction is negligible. However, the electron beam from the trochoidal monochromator has a different overlap with the ion cloud than does the low-resolution beam that was used to measure A'. Therefore in an overlapping range (100–200 meV) points were taken in NO^+ with both guns to determine the new overlap A'' of the high-resolution gun.

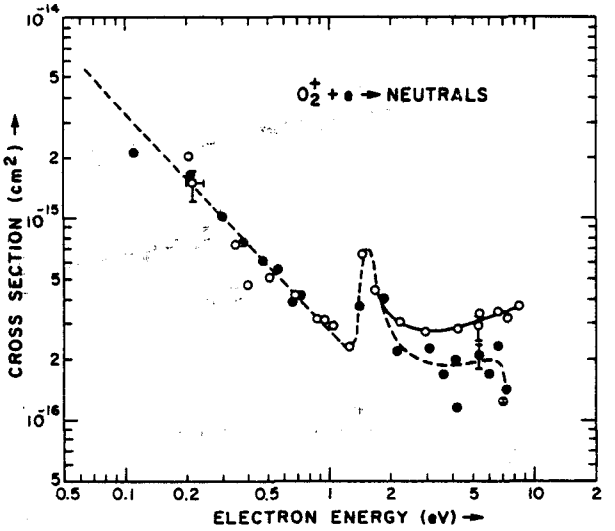

Fig. 2. Measured recombination cross section versus electron energy for O_2^+. Ions produced by 14- and 33-eV electron impact on O_2 are represented by solid and open circles, respectively. The dashed curve was used in equation (3) to obtain a calculated rate coefficient $\alpha_c(T)$.

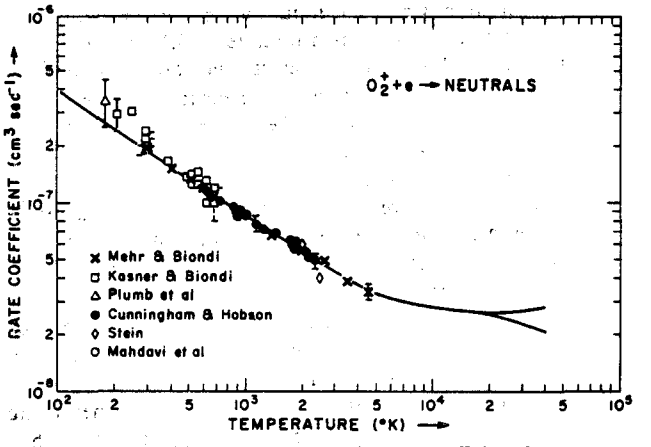

Fig. 3. The solid curves represent the rate coefficient for O_2^+ versus electron temperature calculated from the dashed curve approximation to data in Figure 2. The two curves above 20,000°K show the effect of continuing the cross section in Figure 2 as a constant value above 8 eV (upper curve) or dropping it to zero at 8 eV (lower curve). The error bars have in some cases been moved horizontally (indicated by slanted dashed lines) to keep from obscuring adjacent points.

RESULTS AND DISCUSSION

Cross-section results for O_2^+ are shown in Figure 2. The peak at about 1.5 eV is thought to be due to the opening of a new final state channel for recombination. However, the repulsive levels of O_2^+ are not known well enough for us to make even a tentative channel identification. At 2 eV and above, the shape of the dissociative recombination cross section is distinctly different, depending upon whether the ions were initially created by bombarding O_2 with 14-eV electrons (solid circles) or with 33-eV electrons (open circles). In the case of the 33-eV electron bombardment much of the O_2^+ is probably formed by cascade from excited electronic states of O_2^+ to high vibrational levels of the ground $X^2\Pi_g$ state. This would be concluded from the discussion in the section on the experiment. However, as was noted there, one cannot positively rule out contributions from the $a^4\Pi_u$ state, since the lifetime of this state may be much longer than that guessed.

Rate coefficients calculated by substituting the measured cross section into (3) are shown in Figure 3. For this calculation the measured values are approximated by the dashed curve in Figure 2. The data have been adjusted to determine the overlap A', as was discussed in the section on the experiment. To compute α from (3), it was necessary to extrapolate σ from the lowest-energy value given in Figure 2 to zero energy. The way to do this correctly is not known, although it is suggested (J. N. Bardsley, private communication, 1973) that at some energy the cross section must go to zero energy as $\sigma \sim E^{-1}$. For simplicity we have used various extrapolations of the form $\sigma \sim E^{-n}$ for $1 \leq n \leq 1.4$, and calculated rate coefficients $\alpha_c(T)$ were determined for each case. The curve shown was chosen as the best fit of $\alpha_c(T)$ to the above measurements and was obtained with $n = 1.16$ as is indicated by the dashed line from 0.1 to 1.2 eV in Figure 2. The value of α_c (2000°K) was found to be relatively insensitive to the chosen value of n as well as to the shape of the cross section above 2 eV, and so 2000°K was chosen as the temperature at which A' was determined from (2) and (3). The uncertainty in A' is estimated as 15%, corresponding to an uncertainty of ±0.15 in the choice of n. The values of $\alpha_c(T)$ at very high temperature also depend upon how the cross section behaves past the last measured point in Figure 2. This is illustrated in Figure 3, where the upper curve above 15,000°K is obtained by continuing the cross sections as a constant above 8 eV, whereas the lower curve is obtained by dropping it to 0 above 8 eV. Values of α determined by other workers are shown in Figure 3 and are seen to be in impressive agreement with one another. Calculated $\alpha_c(T)$ from the present data agree satisfactorily with these other measurements over the entire temperature range.

The recombination cross section for NO^+ is shown in Figure 4. Ions were formed from the bombardment of NO by 14-eV electrons. As was discussed earlier, it is assumed that in the long times (~10 min) between the ion formation and the beginning of a measurement, all ions have decayed to the ground electronic and vibrational state. Slope changes or

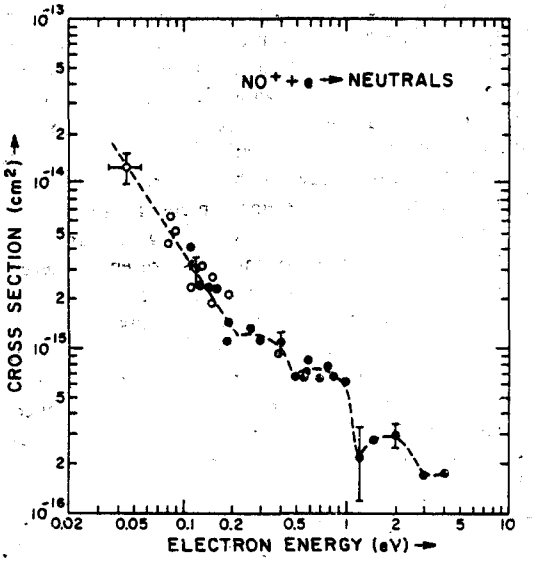

Fig. 4. Measured recombination cross section of NO^+ versus electron energy. Measurements represented by the open and solid circles were taken with the high- and low-resolution electron guns, respectively.

structure in the cross section at about 0.2, 0.4, and 1 eV are taken as evidence that a number of final state channels are involved in the recombination. Flags on the points represent a standard deviation of a measurement and are shown only for representative points. There is also an uncertainty in the ordinate of ±20% from the determination of A'.

Rate constants for NO^+ were calculated by using the dashed line in Figure 4 in (3) and are shown in Figure 5. The dependence of $\alpha_e(T)$ upon the way the cross section is extrapolated to zero energy is exemplified by curves 1 and 2 in Figure 5. Curve 1 was obtained by extrapolating the cross sections to zero energy as $E^{-1/2}$, as is indicated by the dashed line between 0.04 and 0.2 eV in Figure 4. Curve 2 was obtained by extrapolating the cross section as $E^{-1/2}$ down to 0.01 eV and then changing the slope to $1/E$ the rest of the way to zero energy. Curves 3 and 4 show the effects of continuing the cross sections to high energy as a constant or dropping sharply as $1/E^3$, respectively, past the last measured point at 4 eV.

Direct rate coefficient measurements of others [*Mahdavi et al.*, 1971; *Weller and Biondi*, 1968; *Gunton and Shaw*, 1965; *Young and St. John*, 1966; *Stein et al.*, 1964; *Lin and Teare*, 1963], where total temperature is varied, are shown in the plot. Differences in rate coefficients arising because of the difference between electron temperature and total temperature probably would not show up below a few thousand degrees, where vibrational excitation of the ion becomes significant. The position of the Stein et al. and Lin and Teare data points below the present results is not atypical of the predictions of *O'Malley* [1969], *Bardsley* [1968], or *Bardsley and Biondi* [1970] when vibrational excitation of the ions is important. However, when the large uncertainties in these two high-temperature measurements are considered, they are not really in strong disagreement with the present results, and it is questionable whether conclusions should be drawn about the role of vibrational excitation of NO^+ in the recombination process.

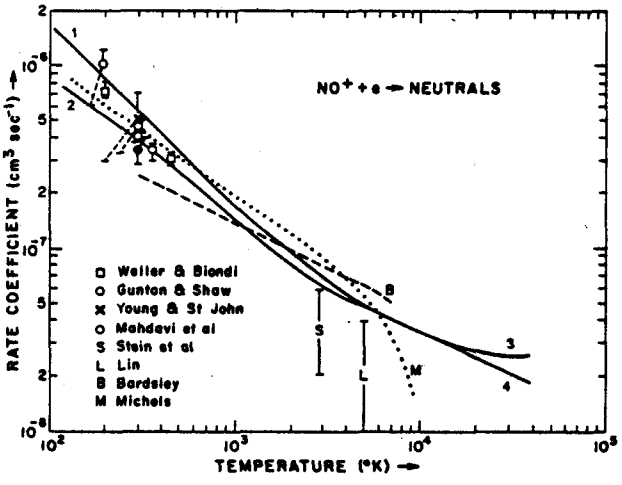

Fig. 5. The solid curves represent rate coefficients for NO^+ versus electron temperature calculated by using equation (3) and the dashed curve approximation to the cross-section data of Figure 4; different extrapolations of the cross-section data to lower (curves 1 and 2) and higher (curves 3 and 4) energies are assumed. For curve 1, $\sigma \propto E^{-1/2}$ for $E \leq 0.2$ eV. For curve 2, $\sigma \propto E^{-1/2}$ for $0.010 \leq E \leq 0.2$, and $\sigma \propto E^{-1}$ for $0 \leq E \leq 0.010$ eV. For curve 3, σ = const for $E \geq 4$ eV. For curve 4, $\sigma \propto E^{-3}$ for $E \geq 4$ eV. The points are the measurements as a function of total temperature. The dashed curve B is a two-state ($B^2\Pi$ and $B'^2\Delta$) calculation of *Bardsley and Biondi* [1970] and *Bardsley* [1968]. The dotted curve M is a three-state ($B^2\Pi$, $B'^2\Delta$, and $^2\Sigma^+I$) ab initio calculation of *Michels* [1973]. The error bars have in some cases been moved horizontally (indicated by dashed slanted lines) to keep from obscuring other points.

Two theoretical calculations of the rate coefficient as a function of electron temperature for recombination of electrons with NO^+ are also displayed in Figure 5. The work of *Bardsley* [1968], and *Bardsley and Biondi* [1970], shown by the dashed curve labeled B, used spectroscopic data to deduce potential curves and took into account the $B^2\Pi$ and $B'^2\Delta$ states. The work of *Michels* [1973] is shown by the dotted curve. He made ab initio calculations of the $B^2\Pi$, $B'^2\Delta$, and $^2\Sigma^+I$ electronic states and took them into account in his recombination calculation. Since Michels also extrapolated his cross sections as $1/E$ below 0.01 eV, they are in that sense analogous to curve 2 of Figure 5. More recent calculations (H. H. Michels, private communication, 1973) include more states and predict a composite cross section with a shape quite similar to that in Figure 4.

Uncertainties in the measurements stem from several sources. The precision of a single cross-section measurement is typically ±20%. The accuracy of the measurement is limited by the uncertainty of 15 → 25% in the overlap A'. The uncertainty in the energy scale of the low-resolution gun is from −10 to +45 meV and is primarily due to uncertainties in the amount of energy in the perpendicular motion of the electrons. For the trochoidal monochromator the uncertainty is ±10 meV. We have analyzed the O_2^+ data with both 0 and 45 meV in the 'perpendicular energy' and have obtained the same value of overlap A' when appropriate path length corrections [*Taylor et al.*, 1974] were also made. The overlap A'' would, however, be increased about 40% if one assumed as much as 45 meV of the perpendicular energy to be present. Roughly, this would have the effect of increasing $\alpha_e(NO^+)$ by 40% below about 1000°K.

Comparison of these experimental results with previous results has been limited in this paper to comparison of rate coefficients, since there are no other direct measurements of cross sections. Comparison with calculated cross sections should be particularly interesting when they become available, since evidence of individual state contributions to the process seems to be evident in the data and should be interpretable with complementary calculations.

Acknowledgments. This work was supported in part by the Atmospheric Sciences section of the National Science Foundation.

* * *

The Editor thanks M. A. Biondi and F. C. Fehsenfeld for their assistance in evaluating this paper.

REFERENCES

Anderson, R., A compilation of measured lifetimes of gaseous diatomic molecules, *At. Data*, *3*, 227–240, 1971.

Bardsley, J. N., The theory of dissociative recombination, *Proc. Phys. Soc. London, Sect. B*, *1*, 365–380, 1968.

Bardsley, J. N., and M. A. Biondi, Dissociative recombination, in *Advances in Atomic and Molecular Physics*, vol. 6, edited by D. R. Bates and I. Esterman, pp. 1–57, Academic, New York, 1970.

Bates, D. R., and G. Poots, Properties of the hydrogen molecular ion, 1, Quadrupole transitions in the ground electronic state and dipole transitions of the isotopic ions, *Proc. Phys. Soc. London, Sect. A*, *66*, 784–792, 1953.

Byrne, J., and P. S. Farago, On the production of polarized electron beams by spin exchange collisions, *Proc. Phys. Soc. London*, *86*, 801–815, 1965.

Cunningham, A. J., and R. M. Hobson, Dissociative recombination at elevated temperatures, 3, O_2^+ dominated afterglows, *Proc. Phys. Soc. London, Sect. B*, *5*, 2320–2327, 1972.

Dehmelt, H. G., and F. L. Walls, 'Bolometric' technique for the rf spectroscopy of stored ions, *Phys. Rev. Lett., 21,* 127–131, 1968.

Gunton, R. C., and T. M. Shaw, Electron-ion recombination in nitric oxide in the temperature range 196 to 358°K, *Phys. Rev., Sect. A, 140,* 756–763, 1965.

Kasner, W. H., and M. A. Biondi, Temperature dependence of the electron-O_2^+-ion recombination coefficient, *Phys. Rev., 174,* 139–144, 1968.

LeFebvre-Brion, H., and F. Guerin, Calculation of the radiative lifetime of the $a^4\Pi$ state of NO, *J. Chem. Phys., 49,* 1446–1447, 1968.

Lin, S. C., and J. D. Teare, Rate of ionization behind shock waves in air, 2, Theoretical interpretations, *Phys. Fluids, 6,* 355–375, 1963.

Mahdavi, M. R., J. B. Hasted, and M. M. Nakshbandi, Electron-ion recombination measurements in the flowing afterglow, *Proc. Phys. Soc. London, Sect. B, 4,* 1726–1737, 1971.

Mehr, F. J., and M. A. Biondi, Electron temperature dependence of recombination of O_2^+ and N_2^+ ions with electrons, *Phys. Rev., 181,* 264–271, 1969.

Michels, H. H., Temperature dependence of dissociative-recombination of $e + NO^+$, in *Electronic and Atomic Collisions, Abstracts of Papers Eighth ICPEAC,* edited by B. C. Cobić and M. V. Kurepa, pp. 891–892, Institute of Physics, Belgrade, Yugoslavia, 1973.

O'Malley, T. F., Theory of dissociative recombination in vibrationally excited gases, *Phys. Rev., 185,* 101–104, 1969.

Plumb, I. C., D. Smith, and N. G. Adams, Formation and loss of O_2^+ and O_4^+ ions in krypton-oxygen afterglow plasmas, *Proc. Phys. Soc. London, Sect. B, 5,* 1762–1772, 1972.

Sayers, J., and L. W. Kerr, Ionic reactions in gases, Proceedings of Third International Conference on Ionization Phenomena in Gases, pp. 908–911, Ital. Soc. of Phys., Vienna, 1957.

Stamatović, A., and G. J. Schulz, Characteristics of the trochoidal electron monochromator, *Rev. Sci. Instrum., 41,* 423–427, 1970.

Stein, R. P., M. Schiebe, M. W. Syverson, T. M. Shaw, and R. C. Gunton, Recombination coefficient of electrons with NO^+ ions in shock-heated air, *Phys. Fluids, 7,* 1641–1650, 1964.

Takayanagi, K., Vibrational relaxation time for molecular ions in gases, *JILA Rep. 17,* 17 pp., Joint Inst. for Lab. Astrophys., Univ. of Colo., Boulder, 1964.

Taylor, P. O., K. T. Dolder, W. E. Kauppila, and G. H. Dunn, Measurement of spiralling in a magnetically confined electron beam for use in collision studies, *Rev. Sci. Instrum., 45,* in press, 1974.

Walls, F. L., and T. S. Stein, Observation of the g-2 resonance of a stored electron gas using a bolometric technique, *Phys. Rev. Lett., 31,* 975–979, 1973.

Weller, C. S., and M. A. Biondi, Recombination, attachment, and ambipolar diffusion of electrons in photo-ionized NO afterglows, *Phys. Rev., 172,* 198–206, 1968.

Young, R. A., and G. St. John, Recombination coefficient of NO^+ with e, *Phys. Rev., 152,* 25–28, 1966.

Zipf, E. C., Jr., The collisional deactivation of metastable atoms and molecules in the upper atmosphere, *Can. J. Chem., 47,* 1863–1870, 1969.

(Received December 26, 1973;
accepted January 30, 1974.)